

## Advances in laboratory acoustic emission study

LEI, Xinglin<sup>1\*</sup>

<sup>1</sup>Geological Survey of Japan, AIST, Japan

Acoustic emission (AE) is an elastic wave radiated by rapid cracking in solids. As a technology of nondestructive inspection, AE has a long history of development and has been applied in numerous areas including material sciences, medical sciences and engineering fields. In stressed rocks, macroscopic fracturing is preceded by a very complex pervasive evolution of some pre-failure damage. Thus, studies focusing on both fracture dynamics and pre-failure damage are a subject of interest and can be inferred from AE statistics as the number of AE events is proportional to the number of growing cracks, and the AE amplitudes are proportional to the length of crack growth increments in the rock. In Earth science, since the similarity in size distribution of earthquakes and acoustic emissions (AE) was found in the 1960s, many laboratory studies have been motivated by the need to provide tools for the prediction of mining failures and natural earthquakes. This report aims to draw an outline of laboratory AE studies in the last 50 years, which have addressed seismological problems, with special focuses on some key issues associated with fault nucleation and growth in brittle rocks.

The AE technique, which monitors the spatiotemporal distribution of AE events, is applied to the analysis of the micro-cracking activity inside the sample space, and it can be performed under an artificially controlled pressure, which is very important for the simulation of underground conditions. During the last five decades, a great number of studies were done following developments in experimental technology, AE monitoring technology, and data processing methodology. Fifty years ago, only the hitting time of an AE could be recorded with a single sensor or a small number of sensors. The rock fracture test was performed under simple loading conditions. Later, the number of sensors that could be used in a study increased and thus allowed the determination of the hypocentre of an AE. Developments in transient memory technique in the 1970s through to the 1980s lead to the ability to make a digital multichannel recording of the full waveform of an AE. Hypocentre location was improved greatly by the use of more precise arrival times obtained through waveform analysis. In addition, it became possible to determine the mode of fracture, i.e., the focal mechanism solution of an AE source. In the present day, AE are usually monitored by 16-32 sensors with digital waveform recording at up to a 200 MHz sampling rate and up to a 16 bit A/D resolution. The dead time of a recording is sufficiently short and continuous recording is possible by use of very large amounts of memory. The waveform of most events can be captured with multiple channels, even for the period of dynamic failure in which the AE rate may reach several thousand a second. Rock fracture experiments can be performed under triaxial compression conditions with controlled fluid injection and pore pressure. AE hypocentres are determined with a location error of a few mms. A focal mechanism solution can be determined for individual events or a group of events. As demonstrated by very recent studies progress in laboratory AE study, particularly studies focusing faulting nucleation, is shedding more and more light on earthquake seismology.

By summarising recent results, it can be concluded that the fault nucleation behaviour, including critical size, duration time, and AE productivity, depend on the heterogeneity of the area of weakness of the fault compared with that of the host rock. If the fault is as strong as the host rock then the fracture makes no difference and the rock remains intact. Furthermore, a homogeneous fault or rock mass appears to fracture in unpredictable ways without a consistent trend in precursory statistics, while inhomogeneous faults fracture with clear precursors related to the nature of the heterogeneity.

Keywords: Acoustic emission (AE), Pre-failure damage, Rock fracture, Earthquake, Fault nucleation, Process zone

## Microfracture distributions indicating formation of large-scale cracks in the rock mass ahead of the mining front

NAOI, Makoto<sup>1\*</sup> ; MORIYA, Hirokazu<sup>2</sup> ; NAKATANI, Masao<sup>1</sup> ; MURAKAMI, Osamu<sup>3</sup> ; THABANG, Kgarume<sup>4</sup> ; THABANG, Masakale<sup>5</sup> ; LUIZ, Ribeiro<sup>6</sup> ; YABE, Yasuo<sup>2</sup> ; KAWAKATA, Hironori<sup>3</sup> ; ANTHONY, Ward<sup>6</sup> ; RAY, Durrheim<sup>4</sup> ; OGASAWARA, Hiroshi<sup>3</sup>

<sup>1</sup>Univ. of Tokyo, <sup>2</sup>Tohoku Univ., <sup>3</sup>Ritsumeikan Univ., <sup>4</sup>CSIR, <sup>5</sup>OHMS, <sup>6</sup>SeismoGen

We are monitoring Acoustic Emissions (AEs) down to Mw -4 or less at 1km beneath the ground in the Cooke 4 Mine (previously known as the Ezulwini Mine), where many earthquakes up to Mw 2 are induced by stress concentration due to tabular mining. The network consists of 24 AE sensors and 6 three-component accelerometers. Naoi et al. (2013; Pageoph) made a catalog composed of about 360,000 events by using waveform data obtained for three months, and reported that 90% of them aggregated within 10 m ahead of the mining front at the time.

In this study, we extended the analysis term to 9 months and developed a catalog composed of about one million events. We also applied the double difference algorithm (Waldhauser and Ellsworth, 2000) to them so as to examine spatial distributions of the AEs near the mining front in detail. Travel time differences for relative location were calculated from arrival times automatically read by the program of Horiuchi et al. (2011). To efficiently calculate relative hypocenters for a massive amount of events, we adopted the parallelization method of Hauksson and Shearer (2005), where events in subregions overlapping each other are firstly relocated and then the hypocenters relocated redundantly are averaged to make a single catalog. We succeeded in relocating 96% of the one million events.

The relocated AEs near the mining front exhibited two-dimensional, tabular aggregations with a few tens of meters lateral extent (hereinafter referred to as tabular cluster), rather than a three-dimensional distribution spread more or less uniformly (randomly) over the entire zone of the stope-front activity of 10 m breadth. Each tabular cluster was discernible because they were separated by regions of low AE density. That is, AEs ahead of the mining front basically occur selectively in several discrete tabular zones within a highly stressed volume affected by the mining cavity. The tabular clusters strike parallel to the mining face and dip 60-80°. This resembles similarly large shear fractures along the plane of maximum shear commonly observed by excavation around the stopes (Gay and Ortlepp, 1979; Adams and Jager, 1980; Adams et al. 1981). Ahead of a panel that advanced by 40 m during the analysis period, 10 such tabular zones formed at intervals of 5 m on average.

By the same AE monitoring network, we also have found extremely aggregated (a few tens of centimeter thickness) planar clusters continuous over the cluster's extent, reminiscent of thoroughgoing fracture surfaces. They often coincide with pre-existing geological faults (Naoi et al. 2013; JpGU). In contrast, the AEs of the tabular clusters regularly forming in the mining front were spread over 1-2 m thickness, lacking a dominant aggregation with good continuity. We interpret that the tabular-cluster AEs are microfractures occurring in a formation process of a large-scale shear crack in macroscopically intact rock subjected to high stress ahead of the advancing mining front. Indeed, the activity of tabular clusters gradually increased as the mining front approached and ceased when passed by the front.

Keywords: Acoustic Emission, Induced Earthquake, Rock fracture

## Deformation and acoustic emission of a penetrated granular bed

MATSUYAMA, Kazuhiro<sup>1</sup> ; KATSURAGI, Hiroaki<sup>2\*</sup>

<sup>1</sup>Department of Applied Science for Electronics and Materials, Kyushu University, <sup>2</sup>Department of Earth and Environmental Sciences, Nagoya University

In general, the rheological behavior of granular matter can mimic a certain side of the geophysical phenomena. In this experiment, the plunged granular matter is used to model the deformation and/or fracturing of the geophysical materials.

Penetration resistant force and acoustic emission (AE) from a plunged granular bed are experimentally investigated through their power-law distribution forms. The experimental apparatus used in this study is basically similar to that in our previous works [1,2]. In this experiment, AE measurement is used to approach the grain's-level microscopic behavior in a penetrated granular bed. An AE sensor (NF AE-9913) is buried in a glass beads bed. Then, the bed is slowly penetrated by a solid sphere by using a universal testing machine (Shimadzu AG-100NX). The average diameter of glass beads is varied from 0.4 to 2 mm, and the penetrating sphere's diameter ranges from 10 to 40 mm. During the penetration, the resistant force applied to the sphere and the AE signal are simultaneously measured [3]. The penetration speed (in the order of 1 mm/s) is kept slow enough to focus on the quasi-static regime. In this slow-penetration regime, the resistant force is independent of the penetration speed. Moreover, the resistant force shows power-law relation to the penetration depth. The obtained power-law exponent seems to depend on the size of granular column, i.e., the container's size. By comparing the resistant forces obtained by this experiment and other experiments, we confirm the relation between the resistant force and container's size. The smaller the container is, the larger the power-law exponent of resistant force becomes. This might mean that the slow penetration drag is affected by side wall of the container through force chains.

For AE signal, we observe a lot of (more than 1,000) burst-like AE events in each penetration experiment. We define the size of each AE event by its maximum amplitude. Then we find that the size distribution of AE events obeys power-law that is similar to Gutenberg Richter's law of the earthquakes statistics. However, the measured power-law exponent is not universal in this experiment. It rather depends on experimental condition. Particularly, the size of beads composing the penetrated granular bed affects the result significantly. The small glass beads bed shows larger power-law exponent. This tendency of power-law exponent indicates that the deformation of small-grains-bed is rather plastic, and the deformation of large-grains-bed shows brittle-like behavior. Namely, the emitted acoustic signal relates to the mode of deformation or fracturing. Since the grains network constructed in a small grains bed is dissipative, it also influences the statistics of AE events. The large AE events could be dissipated and screened by a lot of contact points in the small grains bed. This effect is also consistent with the current experimental result. In this study, only the AE events are measured and analyzed based on its power-law distribution. Actually, to characterize the mode of fracturing more precisely, electromagnetic emission (EME) should be also measured. Simultaneous measurement of AE and EME would reveal the details of the mechanics of slowly penetrated granular bed. Although this result is still preliminary to directly compare the power-law exponent with actual geophysical phenomena, the systematic behaviors of the power-law exponents are qualitatively informative to understand the deformation of the granular matter which relates to various geophysical phenomena and is quite different from usual continuum.

[1] H. Katsuragi, *Material, Chem. Eng. Sci.*, 76, 165-172 (2012).

[2] H. Katsuragi, *Phys. Rev. E*, 85, 021301:1-5 (2012).

[3] K. Matsuyama and H. Katsuragi, *Nonlin. Processes Geophys.*, 21, 1-8 (2014).

Keywords: acoustic emission, quasi-static resistant force, granular matter, power law

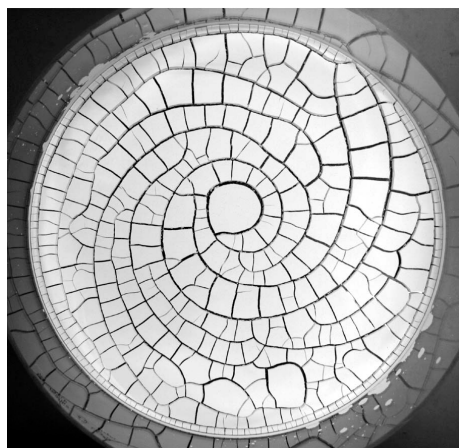
## Variety of memories of clay paste flows which can be visualized as desiccation crack patterns

NAKAHARA, Akio<sup>1\*</sup> ; MATSUO, Yousuke<sup>1</sup> ; OOSHIDA, Takeshi<sup>2</sup> ; OTSUKI, Michio<sup>3</sup> ; KITSUNEZAKI, So<sup>4</sup>

<sup>1</sup>College of Science and Technology, Nihon University, <sup>2</sup>Department of Mechanical and Aerospace Engineering, Tottori University, <sup>3</sup>Department of Materials Science, Shimane University, <sup>4</sup>Graduate School of Human Culture, Nara Women's University

Due to its plasticity, a water-poor clay paste can remember the direction of vibration and flow that it suffered. The memory of flow in clay paste can be visualized as a morphology of crack pattern that appears when the clay paste is dried. When the clay paste remembers the flow direction, desiccation cracks run all parallel to the direction of the flow. Recently, we find that there are some different types of memory of flow, as the direction of crack propagation changes from parallel to perpendicular direction. We would like to discuss on the mechanism of the memory effect of flow.

Keywords: desiccation crack pattern, rheology of clay paste, memory effect of flow



## Precursory Signal of Frontal Thrust Formation: Current status of Large Scale High Precision Sand Box Experiments

HORI, Takane<sup>1\*</sup> ; SAKAGUCHI, Hide<sup>1</sup> ; YAMADA, Yasuhiro<sup>2</sup> ; DOTARE, Tatsuya<sup>2</sup> ; FUKUMOTO, Yutaka<sup>3</sup>

<sup>1</sup>JAMSTEC, <sup>2</sup>Department of Urban Management Engineering, Kyoto University, <sup>3</sup>Graduate School of Agriculture, Kyoto University

In order to find out the mechanism of the three dimensional complex shape formation in sequential thrust and uplift of a accretion prism, we have developed a large scale high precision sand box experimental apparatus since 2011. After a number of modifications in the experimental apparatus and experimental procedure, we finally performed productive runs in July 2013. In specimen preparation, the thickness of a sand layer is controlled with the precision of less than single particle size. As a result, the shape of a frontal thrust became uniformly straight with high reproducibility and no complex shape has been observed since then. However, with such a well-controlled experimental system, we succeeded to detect the precursory signal prior to frontal thrust formation. In this talk, detailed information of the experimental apparatus and our new findings will be given with the scope of applicability of our finding in the field.

Keywords: precursor, earthquake, sandbox experiment

## New modelling devices to enhance the reproducibility of analogue model experiments

DOTARE, Tatsuya<sup>1\*</sup> ; YAMADA, Yasuhiro<sup>1</sup> ; SAKAGUCHI, Hide<sup>2</sup> ; HORI, Takane<sup>2</sup>

<sup>1</sup>Department of Urban Management, Kyoto University, <sup>2</sup>Japan Agency for Marine-Earth Science and Technology (JAMSTEC)

The scaled analogue model experiments have been used for more than 100 years to reproduce the geological development processes in the laboratory scales using the granular material (e.g. dry sand). Recently, we can obtain the small-scale deformation quantitatively by applying digital image analyses. Then, we observed the 'weak shear band' before fault initiation process. However, heterogeneity in the initial model produced by human hand often causes the fluctuation of the experimental results (e.g. fault location, faulting timing and fault geometry).

To solve this problem, we made the experimental device for making the initial model automatically and conducted the experiments to compare the experimental results with the previous method.

We conducted simple convergent experiments. Initial models were made by previous method (human hand) or new method (new device) and experiments were repeated 5 times, respectively.

As a result, while branches of new faults can be seen in the previous method, there are no branches in the new method. In addition, the fluctuation of experimental results was restricted in the new method.

This shows that new experimental device can make the initial model homogeneous and reproduce the same initial model in each experiment.

Keywords: analogue modelling, sandbox, reproducibility, accretionary prism, heterogeneity

## Relaxation processes of granular layer at seismic slip rates and layer thickness.

KUWANO, Osamu<sup>1\*</sup> ; NAKATANI, Masao<sup>2</sup> ; HATANO, Takahiro<sup>2</sup> ; SAKAGUCHI, Hide<sup>1</sup>

<sup>1</sup>IFREE, JAMSTEC, <sup>2</sup>ERI, University of Tokyo

A natural fault has the cataclasite core zone, along which shear deformation concentrates. Rheology of these granular matters thus provides us an important insight in considering the nature of friction on faults from a microscopic point of view. In the past two decades, experiments conducted at sub seismic to seismic slip rates (mm/s to m/s) revealed two remarkable phenomena of high-velocity rock friction; very long critical slip distance ( $D_c$ ) of the order of 1-10m/s and the considerable weakening due to mechanochemical effects by frictional heating [e.g., Di Toro et al., 2011, Nature]. Recently, Chambon et al.[2006, JGR] conducted friction experiment with very large shear displacement experiment on a thick granular layer, and reported significant slip-weakening behavior active over decimetric slip distances. However, the relation between long  $D_c$  observed in a thick granular layer and long  $D_c$  in the high-velocity friction is still not clear. Here, we report on laboratory experiments designed to explore transient responses of a thick granular layer following a step change in slip velocity at seismic slip rates. We use simple particle and choose relatively low normal stress to exclude the possible mechanochemical effects caused by frictional heat. We find that friction coefficient and layer thickness show similar response that is symmetry with respect to velocity changes, and  $D_c$  is of the order of 10m. It appears that these responses are attributed to dynamics of granular matter. We also report how magnitude of the relaxation and  $D_c$  are affected by the layer thickness.

Keywords: high-velocity friction, granular matter, rheology

## Porosity and permeability under effective pressure for the Quaternary Kazusa Group siltstones

MARUMO, Haruna<sup>1\*</sup> ; UEHARA, Shin-ichi<sup>1</sup> ; TAMURA, Yukie<sup>2</sup> ; MITSUHASHI, Shunsuke<sup>2</sup>

<sup>1</sup>Graduate School of Science, Toho University, <sup>2</sup>Faculty of Science, Toho University

The Kazusa group is a geological formation of the middle Pleistocene - Pliocene marine, and widely distributes in middle and northern part of the Boso Peninsula. Mudstones of the Kazusa Group is in the first stage of consolidation (viscous compaction stage), and porosity is 37.9 - 55.5% [1]. In mudstone formations of the Kazusa Group, high porosity anomaly is observed, of which location is consistent with that of natural gas deposits. This high porosity anomaly is suggested to have been generated by an abnormally excess pore pressure. The development process of the high pore pressure is still unknown. Previous studies have discussed the mechanism in connection with production of natural gas, but sufficiently quantitative analyses have not been performed. High pore pressure zone may affect many properties and processes in underground, such as porosity and permeability development in accretionary wedge or sedimentary basins during accretion and depositional process, ground water flows or petroleum migrations in underground, and fault mechanisms. Thus, to elucidate the mechanism of developing the high pore pressure zone is important. We are therefore planning to investigate the mechanism of the high pore pressure zone development by using the 1D model of Tanikawa et al. [2], which include simple deposition and compaction processes. In this study, as the first step of this project, the effective pressure dependences of porosity and permeability were determined for laboratory experiments for siltstone of the Kazusa Group, which are necessary for the modeling.

The measurements were performed using an intra-vessel deformation fluid-flow apparatus at Toho University. The rock samples used in the experiments were collected from outcrops at Umegase Formation, Ota-dai Formation, Kiwada Formation, Ohara Formation and Katsuura Formation of the Kazusa group. The collected samples were shaped into a cylindrical shape about 40 mm in diameter and about 30 mm in height. Distilled water was used for pore fluid and confining pressure was applied by using oil. Permeability and porosity of siltstones were measured at room temperature and under effective pressures from 0 MPa to 35 MPa. To obtain porosity under effective pressure, we measured a volume of water discharged from the specimen when confining pressure was applied. We measured permeability by monitoring flow rate through the specimen under the condition that pore pressure differences at the both side of the specimen is kept constant.

Permeability and porosity ranged from  $10^{-17}$  -  $10^{-18}$  m<sup>2</sup> and to 34 - 42 %, respectively. Permeability and porosity both decreased with increasing effective pressure, and this pressure dependence varies. Based on the results of the experiment, porosity and permeability was expressed in relation to the effective pressure. We have examined the relationship between permeability and porosity.

### References

- [1] Inami, K., Bull. Geol. Surv. Japan 34, 207-216 (1983)
- [2] Tanikawa, W., J. Geophys. Res., 113, B12403 (2008)

Keywords: Kazusa group, porosity, permeability, laboratory experiment

## Rheological properties of mafic schists: Implications for subduction dynamics

OKAZAKI, Keishi<sup>1\*</sup>; HIRTH, Greg<sup>1</sup>

<sup>1</sup>Department of Geological Sciences, Brown University

To understand the spatial and temporal distribution of deformation (e.g., underplating and exhumation of metamorphic rocks) and earthquakes in subduction zones, it is important to constrain the rheological properties of metamorphic rocks (i.e., altered oceanic crust and sediments), and how they evolve during metamorphic reactions following hydration, carbonation and dehydration of the down-going slab. Metamorphism of oceanic crust has stimulated hypotheses on the relationship between intra-slab earthquakes and slab-wedge coupling along plate boundaries in subduction zones. While it is well known that metamorphism has important effects on material fluxes and arc volcanisms at subduction system, it remains unclear how the formation of metamorphic minerals following fluid release influences rheology. Past experimental studies on mafic metamorphic rocks were mostly concentrated on phase equilibrium, thus there are few reports on the mechanical data for these metamorphic rocks.

We conducted triaxial deformation experiments on two mafic schists sampled from the Sambagawa metamorphic belt (Shikoku Island, Japan), using Griggs-type solid pressure- medium apparatus at Brown University. Both mafic schists are mainly composed of amphibole, albite, epidote, and chlorite with small amounts of titanite and phengitic mica. However, there are differences in the peak metamorphic condition (i.e., the maximum PT condition), amphibole composition and mineral abundance of minerals in the two schists. One, which was metamorphosed at greenschist facies (pressure of  $\sim 0.75$  GPa and temperature of  $\sim 400$  °C), has a relatively high chlorite content ( $\sim 12$  %) and actinolite is the dominant amphibole phase. The other, metamorphosed at the epidote-amphibolite facies (pressure of  $\sim 1$  GPa and temperature of  $\sim 520$  °C), has a lower chlorite content ( $< 2$  %) and hornblende is the dominant amphibole phase. Constant strain rate experiments and strain rate stepping experiments were conducted at confining pressures ( $P_c$ ) from 0.76-2GPa, temperatures ( $T$ ) from 300-600 °C and strain rates from  $10^{-5}$ - $10^{-7}$  1/s.

At conditions near the peak conditions of the greenschist ( $P_c = 1$  GPa,  $T = 400$  °C), differential stresses were higher than 1 GPa. The greenschist samples are weaker than the epidote-amphibolite samples under all experimental conditions. Both types of samples exhibit strain rate strengthening; frictional behavior that inhibits earthquake nucleation. Differential stress increased with increasing confining pressure, while friction coefficient decreased with increasing confining pressure and temperature. At  $T = 400$  °C, the nominal friction coefficient ( $\mu$ ) for the greenschist samples was  $\mu \sim 0.34$  at  $P_c = 1$  GPa and  $\mu \sim 0.30$  at  $P_c = 1.5$  GPa; for the epidote-amphibolite,  $\mu \sim 0.48$  at  $P_c = 1$  GPa and  $\mu \sim 0.42$  at  $P_c = 1.5$  GPa. Stress exponents ( $n$ ) for the greenschist samples at  $P_c = 1$  GPa were  $n \sim 26$  at  $T = 300$  °C,  $n \sim 36$  at  $T = 400$  °C and  $n \sim 34$  at  $T = 500$  °C; for the epidote-amphibolite,  $n \sim 31$  at  $T = 400$  °C and  $n \sim 21$  at  $T = 500$  °C. Microstructures of recovered samples showed modest buckling and several localized shear zones. These features suggest that the deformation of mafic schist is accommodated by semi-brittle deformation resulting in strain localization on faults.

We also conducted deformation experiments in which temperature was increased above the thermal stability of chlorite ( $\sim 800$  °C) to simulate a prograde metamorphism in subduction zones. With increasing temperature during deformation, differential stress decreased and reached nearly 0 MPa. This suggests that such reaction-enhanced weakening of metamorphic rocks forms weak fault zones in subducting slab, which might promote detachment of oceanic crust from the subducting slab and allow underplating to forearc crust. The strain-rate strengthening behavior of these materials suggests that such faults would be relatively aseismic.

Keywords: mafic schist, subduction zone, deformation experiment, oceanic crust, semi-brittle deformation, intermediate depth earthquake

## Effect of iron content on the creep behavior of olivine under hydrous conditions

TASAKA, Miki<sup>1\*</sup> ; ZIMMERMAN, Mark<sup>1</sup> ; KOHLSTEDT, David<sup>1</sup>

<sup>1</sup>University of Minnesota

Since iron and hydrogen play important roles in dynamic processes not only in Earth's mantle but also in Mars's mantle, we conducted triaxial compressive creep experiments on polycrystalline samples of olivine,  $(\text{Fe}_{1-x}\text{Mg}_x)_2\text{SiO}_4$ , with  $x = 0, 0.53, 0.77, 0.90$ , and  $1.0$  under hydrous condition. A Paterson-type gas-medium apparatus was used for these experiments. The water contents, determined from Fourier transform infrared (FTIR) spectroscopy analyses of larger  $\text{Fo}_{90}$  crystals embedded in the olivine aggregates, demonstrate that the samples are water-saturated both before and after deformation. The grain sizes of initial and deformed samples were determined using electron backscatter diffraction (EBSD).

Creep tests at 300 MPa confining pressure were conducted at temperatures from 1050 to 1200C at constant stresses in the range 25 to 315 MPa. The values of the pre-exponential term, stress and grain size exponents, and activation energy in the constitutive equation were determined for a wide range of iron concentrations. Samples with high Mg contents are finer grained ( $1-2 \mu\text{m}$ ) than those with low Mg contents ( $10-20 \mu\text{m}$ ). Furthermore, samples with high Mg contents ( $x \geq 0.90$ ) exhibit a stress exponent of  $n = 2$ , whereas samples with low Mg contents ( $x < 0.90$ ) deform with  $n = 3$ . This result is consistent with the dislocation-accommodated grain boundary sliding model of Langdon (1994), which predicts that fine-grained samples that do not contain sub-grains should exhibit  $n = 2$  while coarser-grained samples that do contain sub-grains should exhibit  $n = 3$ . The flow stress decreases with increasing iron content of the olivine samples at constant temperature, strain rate, and grain size. Following the analysis of previous studies (Mackwell *et al.*, 2005; Zhao *et al.*, 2009), we fit our creep data to the following flow law: strain rate =  $A \sigma^n d^{-p} (1-x)^m f_{\text{H}_2\text{O}}^r \exp\{-[Q_0 + \alpha(1-x)] / RT\}$ , where  $A$  is a material-dependent parameter,  $\sigma$  is stress,  $d$  is grain size,  $p$  grain size exponent,  $m$  iron content exponent,  $f_{\text{H}_2\text{O}}$  water fugacity,  $r$  water fugacity exponent,  $Q_0$  activation energy at  $(1-x) = 0$ , and  $\alpha$  a constant. The dependence of strain rate on iron concentration is characterized by two parameters - directly, through the iron content exponent  $m$  and, indirectly, through the term  $\alpha(1-x)$  in the activation energy. The values of  $m$  and  $\alpha$  are determined by the rate-controlling mechanism of deformation and the charge neutrality condition for Fe-bearing olivine.

Keywords: olivine, iron content, creep, rheology, experiments, deformation

## High accuracy measurement of activation energy of creep and electrical conductivity of olivine aggregate

NAKAKOJI, Tadashi<sup>1\*</sup> ; HIRAGA, Takehiko<sup>1</sup> ; MIBE, Kenji<sup>1</sup>

<sup>1</sup>Earthquake Research Institute, The University of Tokyo

It is believed that creep rate of peridotite being major rock in the Mantle is controlled by diffusion of the slowest ion which is  $\text{Si}^{4+}$ . However it is suggested that diffusion of the second fastest ion controls the deformation rate in the system of which not only olivine but it including pyroxene also consists (Sundberg and Cooper (2008)). As seen above, the controlling process has not been understood well. Besides the activation energy being indication for deciding the mechanism is often obtained with a large error range. Therefore, in a case of extrapolating the experimental to the Earth's interior value, the large error will produce a large uncertainty. To solving the two problems, we have conducted the compression experiment and electrical conduction test for olivine simultaneously under a continuously changing temperature.

The sample used for the experiment was synthetic olivine composed of forsterite (90vol %) + enstatite (10vol %), which imitates a material in upper Mantle. To inhibit to grain growth during the experiment, the sample was annealed at 1360 °C for 24 hours in the furnace before the test conducted. During the experiment, the sample was kept loaded at constant stress, 20MPa, and temperature changed from 1360 °C to 1240 °C and then increased from 1240 °C to 1360 °C in order to confirm reproducibility of measurements. Measurement of impedance of the sample was also conducted simultaneously. The sample applied at 20V every ten degree from 1360 °C provided us current response, which was used for measurement of impedance of the sample.

The result of the experimental data provided us viscosity and electrical conductivity of the sample. Viscosity was obtained by the relation of stress and strain rate. Arrhenius plot of reciprocal viscosity shows a linear distribution. This indicates that deformation mechanism of the sample did not change at the applied temperature range in the experiment. Electrical conductivity in the sample was obtained by the resistivity derived from the data by impedance measurement. Assuming that the conduction is thermally-activated process, the relation of conductivity times temperature and temperature shows a linear relation in Arrhenius plot. From each these slopes of lines, Activation energy of  $627 \pm 15$  kJ/mol was obtained about creep and that of  $297 \pm 12$  kJ/mol was obtained about electrical conduction, respectively. This difference of the activation energies indicates that the creep rate and electrical conduction were controlled by different ion or/and different diffusion in the sample.

Sundberg and Cooper (2008) suggested that deformation mechanism is  $\text{Mg}^{2+} + \text{O}^{2-}$  ion diffusion but not  $\text{Si}^{4+}$  diffusion in a case of the sample of olivine + pyroxene. Therefore we compare our result with previous works. Activation energy of lattice diffusion of  $\text{Si}^{4+}$  and  $\text{O}^{2-}$  in olivine are  $\approx 530$  kJ/mol and  $\approx 340$  kJ/mol (Dohmen et al. 2002), respectively and that of  $\text{Mg}^{2+}$  lattice diffusion is about  $400 \pm 60$  kJ/mol (Chakraborty et al. 1994). On other hand,  $627 \pm 15$  kJ/mol was obtained in this study, so that we can infer that lattice diffusion of  $\text{Si}^{4+}$  controlled creep rate. ten Grotenhuis et al. (2004) obtained that activation energy of  $315 \pm 39$  kJ/mol by measuring electrical conductivity of olivine aggregate which has the same composition and almost same grain size of ours, and relation of increase electrical conductivity and decrease in grain size. Consequently, from the grain size is the same one of us, we can infer that grain boundary diffusion of  $\text{Mg}^{2+}$  ion contributed to the conductivity of our sample.

Keywords: olivine, creep, electrical conduction, activation energy, diffusion, polycrystal

## Quantification of grain boundary sliding and grain rotation during diffusion creep of mantle rocks

MARUYAMA, Genta<sup>1\*</sup>; HIRAGA, Takehiko<sup>1</sup>

<sup>1</sup>Department of Earth and Planetary Sciences, Earthquake Research Institute, University of Tokyo

Existence of an anisotropy in the seismic wave velocity in Earth's upper mantle have been known for decades (Tanimoto and Anderson 1984). The seismic anisotropy is often explained by the crystallographic preferred orientation (CPO) of rock-forming minerals, which have anisotropic elasticity. In general, the CPO of olivine produced during dislocation creep is considered to be the primary cause of the anisotropy. Recently, our team showed that the CPO of olivine is produced even during diffusion creep (Miyazaki et al. 2013). However, the mechanism of the CPO development under diffusion creep is still not clear. The purpose of this study is to understand the mechanism in submicron scale by observations of samples surface after the sample deformation where the fine-scale strain markers were imposed.

We used a vacuum sintering technique to synthesize cylindrical samples which were composed of fine-grained forsterite plus 20 vol. % diopside (a combination that we denote Fo80Di20) and forsterite plus 35 vol. % enstatite (En). We polished the lateral side of the sample. Subsequently we imposed grooves on such surface with using a focused ion beam. These marker lines were parallel to the compression axis of sample deformation. We conducted uniaxial compression creep experiments at atmospheric pressure, temperatures of 1300oC and strain rates of  $10^{-5}$  -  $10^{-4}$  s<sup>-1</sup>. After the compression creep experiment, we observed the marker lines under scanning electron microscope (SEM) with field emission gun (JEOL 6500F installed at Nano-Manufacturing Institute, University of Tokyo) to observe how the markers were displaced after the deformation. Such observations allow to quantify the amount of grain boundary sliding and grain rotation due to a plastic deformation of the sample.

We succeeded to observe the marker lines after the deformation. Significant grain boundary sliding was detected from the offsets of the markers at numbers of grain boundaries. No distortion of the markers within the grains was found indicating the absence of intragranular deformation process such as a glide of dislocations. We quantified the grain rotation finding that the rotation angle increases with strain. The average angles in the sample of Fo80Di20 with strain of 3%, 7% and 14% were 1.2°, 3.9°, 6.5°, respectively. We also found larger rotation angle of the grains in Fo80Di20 than in Fo65En35. Fo80Di20 is composed of anisotropic grains of Fo whereas Fo65En35 has isotropic grains, which may explain the difference in the grain rotation between the samples. The shape of anisotropic grains is crystallographically controlled resulting in a development of longer and straight grain boundaries. We assumed that grains were easier to glide at such boundaries resulting in development of CPO during diffusion creep (Miyazaki et al. 2013), which is an modified model of grain rotation during grain boundary sliding creep (Beere 1978). Our present result seems to support our CPO model.

Keywords: grain rotation, grain boundary sliding, CPO, creep

## In-situ observation of crystallographic preferred orientation of olivine deformed in simple shear: Implications for the

OHUCHI, Tomohiro<sup>1\*</sup> ; NISHIHARA, Yu<sup>1</sup> ; SETO, Yusuke<sup>2</sup> ; KAWAZOE, Takaaki<sup>3</sup> ; NISHI, Masayuki<sup>1</sup> ; MARUYAMA, Genta<sup>5</sup> ; HIGO, Yuji<sup>6</sup> ; FUNAKOSHI, Ken-ichi<sup>7</sup> ; SUZUKI, Akio<sup>8</sup> ; KIKEGAWA, Takumi<sup>9</sup> ; IRIFUNE, Tetsuo<sup>1</sup>

<sup>1</sup>Geodynamics Research Center, Ehime University, <sup>2</sup>Department of Earth and Planetary Sciences, Kobe University, <sup>3</sup>Bayerisches Geoinstitut, University of Bayreuth, <sup>4</sup>Earth-Life Science Institute, Tokyo Institute of Technology, <sup>5</sup>Graduate School of Science, University of Tokyo, <sup>6</sup>Japan Synchrotron Radiation Institute, <sup>7</sup>Research Center for neutron Science and Technology, <sup>8</sup>Department of Earth and Planetary Materials Science, Tohoku University, <sup>9</sup>Photon Factory, High Energy Accelerator Research Organization

The characteristics of the seismic anisotropy vary depending on the types of crystallographic preferred orientation (CPO) of olivine. Therefore, the pattern of the seismic anisotropy has been interpreted by taking into account the water- and pressure-induced fabric transitions of olivine in recent studies (Jung and Karato, 2001; Ohuchi et al., 2011). The fabric strength of olivine aggregates is also important when we evaluate the magnitude of the seismic anisotropy in the upper mantle. In the upper mantle, the steady-state fabric strength of olivine is expected to be achieved due to long time-scales of flows.

The dependency of the fabric strength of olivine aggregates on strain has been evaluated in only limited numbers of experimental studies (e.g., Bystricky et al., 2000). Bystricky et al. (2000) showed that total shear strains higher than 4 are needed to achieve the steady-state fabric strength of olivine (D-type fabric) at 0.3 GPa and 1473 K. However, it has been difficult to evaluate the detailed process of the development of fabrics because fabrics of recovered samples have been evaluated. Recently, we have developed experimental techniques for in-situ simple-shear deformation experiments using a D-DIA apparatus. In this paper, we briefly show that our recent experimental results on in-situ observations of stress, strain, and fabric developments in olivine samples.

Simple-shear deformation experiments on olivine aggregates at pressures  $P = 2-3$  GPa, temperatures  $T = 1290-1490$  K, and shear strain rates of  $3E-4$  s<sup>-1</sup> were performed using a deformation-DIA apparatus installed at SPring-8. Shear strain (up to 5) was measured by the rotation of a platinum strain-marker, which was initially placed perpendicular to the shear direction. Differential stress, generated pressure, and CPO patterns of olivine samples were determined from two-dimensional X-ray diffraction patterns using software (IPAnalyzer, PDIndexer, and ReciPro: Seto et al., 2010; Seto, 2012). The CPO patterns of olivine in the recovered samples were also evaluated by the indexation of the electron backscattered diffraction (EBSD) patterns.

A-type olivine fabric was developed under dry conditions. The fabric strength increased with strain ( $<2$ ), and steady-state fabric strength was achieved at shear strains about 2. The [010] axes strongly concentrated to the shear plane normal and its concentration increased with strain. Preferential alignments of the [100] and [001] axes were developed through increase in strain, though concentrations of the [100] and [001] axes were weaker than those of the [010] axes. Development of B-type olivine fabric was observed under wet conditions ( $\sim 700$  ppm H/Si). The fabric strength of B-type sample continuously increased with strain (up to 3). As same as the case of A-type samples, concentrations of the [010] axes were stronger than those of other axes in the B-type sample. Because the concentration of the [010] axes efficiently increases at strains larger than 1, seismic anisotropy (e.g.,  $V_{SH}/V_{SV}$ ) at shear strains = 1 is quite similar to that under the steady-state conditions.

Using the CPO data of the steady-state A-type fabrics,  $V_{SH}/V_{SV}$  of the asthenospheric upper mantle is estimated to be 1.027 (note that 70 vol.% of preferred-orientated olivine grains and 30 vol.% of random-orientated orthopyroxene grains are assumed in the calculation). This value is consistent with the global one-dimensional model reported by Visser et al. (2008). The  $V_{SH}/V_{SV}$  of the asthenospheric upper mantle is expected to have higher values in the case of B-type fabric (e.g., 1.035), which is harmonious with the global one-dimensional model reported by Panning and Romaniwics (2006). Our results show that seismic anisotropy in the upper mantle is mostly explained by the steady-state olivine fabrics (A- and B-types), and other effects (e.g., shape-preferred orientation of melt, CPO of other minerals) would be limited.

Keywords: olivine, crystallographic preferred orientation, in-situ observation, seismic anisotropy

## Simultaneous observations of dehydration and AE activities during the deformation of antigorite at high pressures

IWASATO, Takuya<sup>1\*</sup>; KUBO, Tomoaki<sup>1</sup>; HIGO, Yuji<sup>2</sup>; KATO, Takumi<sup>1</sup>; KANESHIMA, Satoshi<sup>1</sup>; UEHARA, Seiichiro<sup>1</sup>; IMAMURA, Masahiro<sup>1</sup>

<sup>1</sup>Kyushu Univ., <sup>2</sup>JASRI

Intermediate-depth earthquakes are seismic activities at depths of 60-300 km, where subducting plates deform plastically rather than brittle failure. Because dehydration embrittlement (Raleigh and Paterson, 1965) may not work for serpentinite at pressures more than ~2 GPa, it is important to understand the mechanisms of shear instability at higher pressure. To conduct simultaneous observation of dehydration reaction, plastic flow and shear instability, we developed an in-situ observation system combined with synchrotron monochromatic X-ray and AE 6-6 system (multiple acoustic emission measurement for multi-anvil 6-6 type system) using Deformation-DIA (D-DIA) apparatus. Using this system, we carried out antigorite deformation experiments up to ~4.5 GPa and ~850 K including the condition of the antigorite dehydration to talc and forsterite.

Deformation experiments were conducted at high pressure and high temperature using a 1500-ton uniaxial press (SPEED Mk. II) with a D-DIA type guide block installed at BL-04B1, SPring-8 (Katsura et al., 2004; Kawazoe et al., 2011). 50 keV monochromatic X-ray were used to measure two-dimensional X-ray diffraction (2D-XRD) patterns and X-ray radiography images, which give reaction kinetics, differential stress, and strain. We developed MA 6-6 type system (Nishiyama et al., 2008) to monitor shear instabilities by AEs from maximum six piezoelectric devices positioned between first and second stage anvils. AE waveforms were recorded in trigger mode using six-channel 8-bit digital oscilloscopes at a sampling rate of 50MHz. Starting material of polycrystalline antigorite cylinder (1.7 mm in diameter and 2.7 mm in length) cored from high-temperature serpentinite (Eigami, Nagasaki, Japan) were first compressed at room temperature, then heated at constant load, and finally deformed with constant strain-rate mode. In some runs, dehydration occurred during heating or deformation. Microstructures of recovered samples were preliminarily observed by optical microscopy.

A total of ten deformation experiments of polycrystalline antigorite were conducted at 1.1~4.5 GPa, 300~850 K, and strain rates of  $3.4\sim 6.7 \times 10^{-5} \text{ s}^{-1}$ . AEs were frequently generated from the sample during the cold compression. Relatively large AEs were also detected when heating the sample to 673 K, while AE activities became zero at higher temperatures. During the constant strain-rate deformation, the flow stress reached steady state at the sample strain of more than 5%, and no stress drops were observed until the final strain of ~30-40%. These flow behaviors and the flow strength are almost consistent with the previous study (Hilaret et al., 2007). We also detected AEs during the deformation stage although the frequency was lower compared to the cold compression and heating stages. The AE activities during the deformation became large at lower temperature and larger strain conditions. Optical microscopic observation revealed that some faults are present in the antigorite samples recovered from each stage. On the other hand, we observed dehydration reaction from antigorite to talc-like phase during the deformation at 800 K. The reaction was very slow and only one AE event was detected at the strain of ~25%. Because the faults were only observed in the relict antigorite region, the AE was possibly originated from antigorite. At higher temperature of 850 K, complete dehydration quickly occurred before the deformation. No AEs were detected during the dehydration and the following deformation of dehydrated materials to more than 30% strain. No faults were observed in the recovered sample. Our simultaneous observations of reaction and AE activities showed that the AE is not generated by dehydration of antigorite at more than ~2 GPa. Instead, the unstable fault slipping that generates AEs occurs during heating and deformation of antigorite without dehydration.

Keywords: Acoustic emission, In situ X-ray observation, deformation-DIA, antigorite, dehydration, stress and strain

## Seismic attenuation measurement by cyclic loading under high pressure and temperature

YOSHINO, Takashi<sup>1\*</sup> ; YAMAZAKI, Daisuke<sup>1</sup> ; HIGO, Yuji<sup>2</sup> ; FUNAKOSHI, Ken-ichi<sup>3</sup>

<sup>1</sup>Institute for Study of the Earth's Interior, Okayama Univ., <sup>2</sup>JASRI, <sup>3</sup>CROSS

The estimation of the mantle structure using seismic tomography method has been advanced by understanding of the detailed velocity structure of the Earth interior. On the other hand, Brillouin scattering in the DAC at very high pressure, X-rays inelastic scattering, sound velocity measurement of ultrasonic range in the large press is also improved. These developments can be expected this time as a further declaration of a picture of a more detailed Earth interior. However, as compared to the frequency band of MHz to GHz region, the frequency range of the seismic waves propagating through the earth interior is much lower. We should noted that it is greatly affected by the attenuation of seismic waves. Because the materials are not in a perfectly elastic body, energy loss inside the materials occurs in the wave propagation because of presence of grain boundaries, dislocations, and defects. Thus, seismic attenuation occurs as a function of frequency.

The attenuation of seismic waves (the determination of the  $Q^{-1}$ ) of mantle material under high pressure has not been reported until recently mostly because it is an experimental quantification is very difficult. Temperature effects and particle size effects were reported for the first time systematically for olivine aggregates at high temperature under low pressure. However, for this system the upper limit of the generated pressure is low because it is a torsion test performed in the gas pressure. So the study of pressure -dependent and high-pressure mineral is difficult. The other group using the D-DIA type press having two differential ram measured  $Q^{-1}$  combining an in-situ observation and radiation uniaxial periodic vibration test. This system expands a possibility of experimental determination of  $Q^{-1}$  at much higher pressure. In Japan, the DIA type press was installed at SPring8 (D-DIA). Recently we started the measurement of  $Q^{-1}$  under high pressure using in situ image acquisition of the high time and spacial resolution at short period of oscillation cycle.

In this paper, some experimental developments for measuring seismic attenuation at high pressure and results of cyclic loading tests are introduced. Time resolved images of the sample and reference material obtained by a synchrotron X-ray radiography provide their strain as a function of time during cyclic loading. Attenuation is determined as the tangent of the angle of phase lag between the strain of the sample and the strain of the reference material. A newly installed short period sinusoidal cyclic loading oil pressure system enable us to determine minimal strain of the sample in a wide frequency range from 2 to 0.01 hertz on olivine aggregates at 1 GPa and up to 1673 K. The detectable minimum strain is around  $5 \times 10^{-5}$ . Several test experiments exhibited resolvable  $Q^{-1}$  ( $10^{-2}$ ) above 1273 K. The results are generally consistent with previously reported data.

Keywords: seismic attenuation, high pressure, oscillation, Q value, shear modulus

## Viscoelastic property of antigorite

YAMAZAKI, Daisuke<sup>1\*</sup>

<sup>1</sup>Okayama University

Seismological data reveals the structure and dynamics combined with mineral physics. For example, the velocity structures from observations are interpreted using the elastic properties of constituting minerals obtained from the laboratory measurements. Because the minerals in the earth is not perfect single-crystal but they contain a certain amount of defects (vacancy, dislocation, grain boundary), the viscoelastic relaxation is taken place by the viscous motion of the defects during the propagating the seismic waves with the frequency of  $10^{-4}$ -10 Hz. Serpentine can be considered to be one of the candidate for the source of the fluid in the wedge mantle. In the present study, therefore, we examine the viscoelastic property of serpentine (antigorite) under uppermost mantle conditions by means of high pressure experiments.

Fine-grained polycrystalline antigorite (a few micrometer of grain size) sintered at 3 GPa and 550 degree C for 4 hours was used as a starting material for the attenuation experiment. We conducted the experiments by using D-DIA press with a short-period cyclic loading system, which was recently installed at BL04B1, SPring-8, Japan. D-DIA, which is a single stage of six-anvil compression device, applied pressure by forcing each of the six anvils to advance on the cubic pressure medium with a main ram. After pressure reaching to the target value of 1 GPa by the pumping the main ram, a sinusoidal stress and strain was applied by advancing and withdrawing the upper and lower anvils operated by the short-period cyclic loading system with the frequency between 0.01-2 Hz at 1 GPa and 500-750 degree C. At high temperature ( $> \sim 650$  degree C), dehydration is expected. The strain was monitored directly from X-ray radiography of sample located in the pressure medium through the anvil gap during cyclic loading. In the present study, single crystal of forsterite was placed next to the sample along the stress axis of the sample and it can be used as the standard to estimate the stress by recording the X-ray radiography images displaying the lengths of standard and sample simultaneously.

The time lag of strain of sample against that of standard provided us the quality factor,  $Q$ , to be 5.4, 4.8 and 4.4 for the periods of 5, 10 and 20 s, respectively, at 600 degree C. Present preliminary results shows the temperature dependence of  $Q^{-1}$ . At 500 degree C,  $Q^{-1}$ s are  $\sim 0.5$  log unit lower than those at 600 degree C. The present values is  $\sim 2$  order of magnitude lower than that of olivine aggregates. The shear modulus was estimated to be 15-25 GPa in our experimental condition, which is much smaller than the shear modulus without attenuation (38.5 GPa). The large reduction in shear modulus due to attenuation was previously reported in the case of olivine.

## Experimental study of anelasticity of a polycrystalline material near the melting temperature

YAMAUCHI, Hatsuki<sup>1\*</sup>; TAKEI, Yasuko<sup>1</sup>

<sup>1</sup>Earthquake Research Institute, University of Tokyo

Rock anelasticity is important to interpret seismic wave velocity and attenuation structures in the upper mantle. By using organic polycrystalline borneol ( $C_{10}H_{18}O$ , melting temperature = 204.5 °C) as an analog to mantle rock, McCarthy et al. (2011) measured Young's modulus and attenuation  $Q^{-1}$  as functions of frequency  $f$  ( $=10^{-4}$  - 2 Hz), temperature  $T$  (20-50 °C) and grain size  $d$  (3.3 - 22 micrometer). They also measured viscosity, and calculated the Maxwell frequency  $f_m$ . When the obtained  $Q^{-1}$  spectra were plotted as functions of the frequency normalized by the Maxwell frequency  $f_m$ , all  $Q^{-1}$  spectra obtained for various temperatures and grain sizes collapsed onto a nearly single curve. Moreover, data from olivine aggregates (Gribb and Cooper, 1998; Tan et al. 2001; Jackson et al. 2002) collapsed onto the same master curve as borneol, demonstrating the universality of anelastic behavior. However, experimental frequencies normalized by the Maxwell frequency of the samples were lower than  $5 \times 10^4$ , which is considerably lower than those of seismic waves in the upper mantle ( $f/f_m = 10^6$ - $10^9$ ). Therefore, whether the Maxwell frequency scaling is applicable to the seismic waves or not is an open question.

Takei et al. (in preparation) measured anelasticity of organic polycrystalline borneol at lower temperatures (0-20 °C) and higher frequencies ( $10^{-4}$ -50 Hz) than McCarthy et al. (2011). They also investigated the effect of chemical composition on anelasticity, by using the samples made of high-purity borneol and borneol + diphenylamine ( $(C_6H_5)_2NH$ ) (eutectic temperature = 43 °C). Before obtaining these data, our experimental methodology and data quality were much improved. When the obtained  $Q^{-1}$  spectra were plotted as functions of the frequency normalized by the Maxwell frequency, the  $Q^{-1}$  spectra collapsed onto a nearly single curve at  $f/f_m < 10^4$ , but significantly scattered at  $f/f_m > 10^4$ , where the spectra have a broad peak and the scattering is caused by the variation of the peak amplitude and width with temperature, grain size and chemical composition. Therefore, the simple Maxwell frequency scaling is not applicable to the seismic waves in the upper mantle. They found that seismic attenuation predicted from the data of high purity samples and those of the borneol + diphenylamine samples under low temperature conditions is too low to explain the seismic attenuation in the upper mantle ( $\sim 0.01$ ). In other words, enhancement of attenuation near the melting temperature is important to understand high  $Q^{-1}$  in the upper mantle.

In this study, we measured anelasticity of borneol + diphenylamine system at various frequencies ( $2 \times 10^{-4}$  - 50 Hz) and temperatures (20 - 46 °C), and obtained the detailed behavior of anelasticity near the melting temperature (43 °C). The result obtained so far show that the change of viscosity and anelasticity near the melting temperature is not discrete but continuous. This result is somewhat different from our previous understanding that physical properties abruptly change when melting starts beyond the solidus. We will further obtain systematic data for various grain sizes and melt fractions.

Keywords: anelasticity, seismic attenuation

## Experimental study of bulk and shear viscosities of partially molten rock analogue

SUZUKI, Ayako<sup>1\*</sup> ; TAKEI, Yasuko<sup>1</sup> ; WATANABE, Shun-ichi<sup>2</sup>

<sup>1</sup>Earthquake Research Institute, University of Tokyo, <sup>2</sup>Hydrographic & Oceanographic Dept, Japan Coast Guard

Deformation of partially molten rock is controlled by two independent viscosities: shear viscosity for shear deformation and bulk viscosity for compaction/decompaction. Bulk viscosity and its ratio to shear viscosity,  $h_b/h_s$ , play an important role in melt segregation dynamics in the upper mantle (Katz, 2008). However, that value has not been well constrained theoretically nor experimentally especially at small melt fractions. Most numerical studies have used the theoretically predicted value of  $h_b/h_s = \sim f^{-1}$ , where  $f$  is the melt fraction. Takei and Holtzman (2009a) theoretically obtained a constant value of  $h_b/h_s$  by taking into account a diffusion creep mechanism. The discrepancy between two models is significant at small melt fractions. There has not been experimentally determined value of  $h_b/h_s$  because very few experimental studies have been done about bulk viscosity although shear viscosity has been measured extensively. To discuss the validity of these models based on the experimental data, it is highly important to measure both bulk and shear viscosities by using the equivalent samples. In this study, we measured experimentally these two viscosities as functions of melt fraction using a partially molten rock analogue.

Samples were polycrystalline aggregates of borneol-diphenylamine binary with eutectic temperature of 316K, which has a quite similar equilibrium microstructure to olivine + basalt system (Takei, 2000). Initial melt fraction can be controlled precisely by the concentration of diphenylamine because of its simple eutectic reaction. Before deformation experiments, samples were annealed at 320K for  $\sim 100$  hours in a sealed capsule to make those grain size large enough ( $\sim 0.030$  mm), resulted in negligible grain growth during the successive deformation tests at the same temperature.

To measure bulk and shear viscosities, we carried out two separate experiments. For bulk viscosity, compaction experiments were performed under the diffusion creep regime. A cylindrical sample was compacted uniaxially in a rigid sleeve ( $e_{zz} < 0$ ,  $e_{xx} = e_{yy} = 0$ , where  $e$  is the strain). Melt was squeezed out from the partially molten sample into porous metals which contact with the sample at the top and bottom ends until melt fraction becomes nearly zero. Evolution of melt fraction in the sample was calculated from the sample length measured with digital gauge. Apparent viscosities as a function of melt fraction were proportional to  $\exp(-af)$  with  $a = \sim 30$  at  $f > 4\%$ , which is quite consistent with the olivine + melt systems (Renner et al., 2003). At  $f < 3\%$ , deviation of the viscosity from the exponential curve occurs, suggesting the possible effects of permeability and change of rate limiting process of the volumetric creep (Takei & Holtzman, 2009b). For shear viscosity, uniaxial deformation experiments were performed without a horizontal confining pressure ( $s_{zz} < 0$ ,  $s_{xx} = s_{yy} = 0$ , where  $s$  is the stress). Melt fraction was nearly constant during the test. Deformation tests were conducted with some constant load steps under the diffusion creep regime. Apparent viscosity is evaluated from the stress and the strain rate at steady state.

From the two apparent viscosities obtained independently, we can calculate each bulk and shear viscosities as functions of melt fraction. We will test the predictions of models and discuss the possible viscosity ratio of the partially molten rocks in the upper mantle.

### References:

- Katz RF (2008) J.Petrol., 49, 2099-2121.
- Renner J, Viskupic K, Hirth G, Evans B (2003) G<sup>3</sup>, 4, doi:10.1029/2002GC000369.
- Takei Y (2000) JGR, 105, 16665-16682.
- Takei Y, Holtzman BK (2009a) JGR, 114, doi:10.1029/2008JB005850.
- Takei Y, Holtzman BK (2009b) JGR, 114, doi:10.1029/2008JB005851.

Keywords: viscosity, bulk viscosity, shear viscosity, partial melt

## Role of Mg-O grain-boundary diffusion in rheology and grain-growth in the Earth's mantle

NISHIHARA, Yu<sup>1\*</sup> ; NISHI, Masayuki<sup>1</sup> ; MARUYAMA, Genta<sup>2</sup>

<sup>1</sup>Geodynamics Research Center, Ehime University, <sup>2</sup>Earthquake Research Institute, University of Tokyo

Material and heat transports in the Earth highly depends on rheology and grain-growth kinetics of the constituent materials. Although rheology and grain-growth in single phase aggregate have been studied extensively, knowledge of those in multi-phase system is still limited. Sundberg and Cooper (2008) pointed out the importance of a creep mechanism in which strain is produced by Mg-O grain-boundary diffusion accompanied with reaction at olivine-orthopyroxene phase boundary in the Earth's upper mantle. Tasaka and Hiraga (2013) showed that grain-growth in forsterite-enstatite two-phase system is rate-limited by growth of secondary phase through Mg-O grain-boundary diffusion. These reports suggest that Mg-O grain-boundary diffusion plays important role both in rheology and grain-growth. Recently, our group reported Mg-O grain-boundary diffusion coefficients in forsterite and MgSiO<sub>3</sub> perovskite (Maruyama et al., 2013; Nishi et al., 2013). In this study, theoretical model using our Mg-O grain-boundary diffusion data are compared with available rheological and grain-growth data, and importance of these mechanisms are discussed.

Flow-law were calculated for Mg-O grain-boundary diffusion creeps accompanied by reaction at forsterite-enstatite phase boundary (upper mantle) or accompanied by grain-growth of periclase (lower mantle) using Coble's (1963) equation and results by Maruyama et al. (2013) and Nishi et al. (2013). The derived flow-law for the upper mantle shows ~3 orders of magnitude faster strain-rate than that of creep experiments by Tasaka et al. (2013) which suggests this mechanism is not realistic. Although no comparable creep data was reported for the lower mantle, the derived flow-law shows faster strain-rate than that by Si lattice diffusion creep that was assumed in Xu et al. (2011) and the mechanism is a possible candidate deformation mechanism in the most part of lower mantle.

Grain-growth in the forsterite-enstatite two phase system was studied by Tasaka and Hiraga (2013) experimentally and it is already shown that grain-growth in this system is rate-limited by growth of secondary phase through Mg-O grain-boundary diffusion. Based on the same manner as Tasaka and Hiraga (2013), grain-growth law was calculated for the lower mantle assemblage MgSiO<sub>3</sub> perovskite-periclase system using Ardell's (1972) theory and Nishi et al.'s (2013) results. Derived grain-growth law was generally consistent with the grain-growth data in MgSiO<sub>3</sub> + MgO system reported by Yamazaki et al. (1996). Yamazaki et al.'s results can be explained by initial rapid growth from metastable texture and subsequent normal grain-growth which is rate-limited by Mg-O grain-boundary diffusion. Based on this interpretation, grain-size in the lower mantle is estimated to reach several hundred micro meter by 10<sup>6</sup> years.

Keywords: Upper mantle, Lower mantle, Rheology, Grain-growth, Olivine, Mg-perovskite

## Relationship between Skempton's coefficient and diagenesis of the Quaternary Kazusa Group siltstones

MITSUHASHI, Shunsuke<sup>1\*</sup> ; UEHARA, Shin-ichi<sup>1</sup> ; MARUMO, Haruna<sup>2</sup> ; TAMURA, Yukie<sup>1</sup>

<sup>1</sup>Faculty of Science, Toho University, <sup>2</sup>Graduate School of Science, Toho University

Skempton's coefficient  $B$  is one of fundamental properties of sediments and rocks.  $B$  is defined as the change in pore pressure per unit change in total stress applied under undrained conditions. To reveal the evolution of  $B$  of sediments and sedimentary rocks during diagenesis is critical for some processes relating to geophysics and geology, such as mechanisms of developing abnormal pore pressure in sedimentary basins (Tanikawa et al., 2008). However, how  $B$  depends on diagenesis is still not clear. To understand the dependency, we evaluated  $B$  based on porosity measurements under effective stress for siltstones collected from various formations in the Quaternary Kazusa Group. We also tried to measure  $B$  directly, and compared the results with  $B$  values obtained from measurements of porosity.

We used siltstones of Umegase, Otadai, Kiwada, Ohara and Katsuura Formations of the Kazusa Group as the samples for the experiments. The specimens from the samples were 30 mm in diameter and 40 mm in length. The laboratory experiments were performed using an intra-vessel deformation fluid-flow apparatus at Toho University, at room temperature and under confining pressures from 2 MPa to 35 MPa. Distilled water was used for pore fluid. From the results of the porosity measurements under effective pressure, we estimated the compressibilities of the rock on the assumption that volume change of the rock at effective stress change equals to the pore volume change, and calculated  $B$  from the results. In the direct measurements of  $B$ , we measured pore pressure changes when confining pressure were applied under undrained conditions.

The results of  $B$  estimations from porosity measurements indicated that  $B$  tends to decrease with increasing burial depth. But,  $B$  of Ohara siltstones was somewhat higher than other samples despite Ohara Formation is relatively lower in the Kazusa Group. This is probably because siltstones at Ohara Formation were not consolidated enough as compared with those at other formations due to some reasons such as developing abnormal pore pressure. Results indicated that the dependency of  $B$  on effective pressure is not simple.  $B$  was not simply decreased with effective pressure increases, but  $B$  was increased at some range of effective pressure, which mostly reflected that the compressibility was increased at the transition from overconsolidation to normal consolidation state.  $B$  depends on both compressibility and porosity, and in the case of the Kazusa Group siltstones, the behavior of compressibility has greater effect on  $B$ . Thus,  $B$  is decreased as a grade of diagenesis increases because compressibility is decreased. The values of  $B$  measured directly tended to be higher than  $B$  estimated from measurements of porosity. This is probably because a period between step changes of effective stress was not enough for the rocks to reach steady state.

Keywords: Skempton's coefficient, diagenesis, Kazusa Group, porosity, compressibility, laboratory rock experiment

## Effects of pore pressure changes on frictional behaviors of talc

UEHARA, Shin-ichi<sup>1\*</sup>; OKAZAKI, Keishi<sup>2</sup>; SHIMIZU, Ichiko<sup>3</sup>

<sup>1</sup>Faculty of Science, Toho University, <sup>2</sup>Department of Geological Science, Brown University, <sup>3</sup>Faculty of Science, The University of Tokyo

Since the discovery of low frequency earthquake, several classes of physical mechanisms have been proposed to explain this events. Several models and geophysical observations have suggested that the overpressurized fluid along the subducting plate interface have an important role in triggering such events. In addition, the existence of hydrous minerals along the plate boundary at fore-arc wedge may also be important for the seismogenic properties of the slab-mantle interface. Especially, serpentine minerals are generally expected to be the main hydrous mineral present in the fore-arc minerals, and the existence of serpentine in the wedge mantle has suggested by seismological studies. However, talc may also be important in fault mechanism at the plate boundary in the fore-arc wedge mantle, because slab-derived fluids are likely to lead replacement of serpentine by talc at the slab-mantle interface in the fore-arc wedge mantle, and talc is one of the weakest minerals that constitute natural fault zones. However the quantitative influences of pore pressure on the frictional properties of talc are not well constrained. We conducted friction experiments using pre-cut samples of talc with controlling pore pressure  $P_p$  and confining pressure  $P_c$  adopting several kinds of stress paths during an experiment.

Cylindrical samples of talc (Gvangjsih, China), 20 mm in diameter, were cut at an angle of  $30^\circ$  to the sample axis. The sliding surfaces were ground with carborundum (#400). A small hole (3 mm in diameter) through the center of each piece ensured adequate communication of the water between the pre-cut surfaces with the rest of the pore pressure system. The specimen was loaded by a triaxial apparatus and sheared under an axial displacement rate of  $1 \mu\text{m/s}$ . We used water as a pore fluid. All measurements were performed at room temperature. Experiments were conducted under several paths of  $P_c$  (up to 110 MPa) and  $P_p$  (up to 100 MPa). During steady axial loading, either  $P_c$  or  $P_p$  was changed stepwise.

The stepwise changes of effective normal stress  $\sigma (= \sigma_t - P_p$ , where  $\sigma_t$  is total normal stress) resulted in a linear elastic response of shear stress followed by a transient evolution of friction. In the case that  $\sigma$  was decreased, friction coefficient  $\mu$  was temporally increased and then decreased back to steady state, and the normalized transient change of  $\mu$  to the logarithm of normalized amplitude of  $\sigma$  change ranged from 0.2 to 0.28, which is comparable to that for quartz and Westerly granite reported by previous studies (Linker and Dieterich, *J. Geophys. Res.*, 1992; Hong and Marone, *Geochem. Geophys. Geosyst.*, 2005). While in the case that  $\sigma$  was increased ( $\mu$  was temporally decreased then increased), the values were smaller (less than 0.12, and negative in some cases), which means that a transient change of  $\mu$  was less dependent on a change of  $\sigma$  than that for quartz and granite, which may reflect ductile deformation of contacts on fault surfaces during the evolutionary transition.

This frictional property might cause slow slip phenomena. After an initiation of a fault slip, possibly triggered by an increase of pore pressure, partially undrained conditions on the slip surface may cause dilatancy hardening, and therefore  $\sigma$  may be increased during the slip. The results of this study suggest that, in the case that a fault plane is covered by talc, the temporal decrease of  $\mu$  following an increase of  $\sigma$  might be smaller than the case that fault planes are covered by other ordinary minerals. Consequently, a frictional resistance might act more effectively than faults covered by other ordinary minerals and an acceleration of fault slip rate might be mitigated, and therefore a slip rate might be smaller than regular earthquakes.

This research is supported by Grant-in-Aid for Scientific Research on Innovative Areas, KAKENHI.

Keywords: talc, friction experiment, pore pressure, low frequency earthquake

## Sintering experiments on fine-grained polycrystalline orthoclase

OHIRA, Akane<sup>1\*</sup> ; ISHIKAWA, Masahiro<sup>1</sup>

<sup>1</sup>Graduate school of Environment and Information Sciences, Yokohama National University

K-feldspar is one of the major mineral components of granitic rocks and a wide variety of metamorphic rocks. Its deformational behavior is important for establishing the overall rheology of continental crust. The creep strength is influenced by various factors such as mineral species, grain size and pores. Therefore control of these factors in polycrystalline minerals is essential for rheological experiments. In order to make dense polycrystalline orthoclase, we have carried out sintering experiments.

We prepared submicron mineral powders from a single crystal of orthoclase ( $K_{0.83}Na_{0.17}Al_{1.04}Si_{2.96}O_8$ ). As a result of X-ray fluorescence (XRF) analysis,  $ZrO_2$  (<5.65wt.%) which is considered to be contamination from a mill was detected. We formed cylindrical compacts from fine-grained mineral powders by uniaxial dry pressing at room temperature and pressure of 20MPa. Sintering was carried out using a tube furnace at temperature of 970 °C for 4 hours, achieving a vacuum condition of  $\sim 4.1 \times 10^4$  Pa. We also compared the sintered body with a sample sintered at atmospheric pressure using muffle furnace at the same temperature and the time. Sintered bodies were observed using scanning electron microscope (SEM), and analyzed by XRF and X-ray diffraction (XRD).

As the result of vacuum and atmospheric pressure sintering, we obtained sintered bodies with volume reduction of 52.2% and 44.5%, and porosity of 0.15 and 0.17, respectively. SEM images showed that densification process was advanced by both vacuum and atmospheric pressure sintering. We confirmed that crystal structures (Al/Si order-disorder) were not changed from compacts by XRD patterns.

In this study, we found that dense submicron polycrystalline orthoclase can be made from fine-grained powders by either of vacuum and atmospheric pressure sintering, and confirmed that orthoclase does not cause order-disorder phase transition by a sintering for 4 hours.

Keywords: submicron, orthoclase, sintering

## Doping effect on high-temperature creep of polycrystalline anorthite

YABE, Kosuke<sup>1\*</sup> ; KOIZUMI, Sanae<sup>1</sup> ; HIRAGA, Takehiko<sup>1</sup>

<sup>1</sup>Earthquake Research Institute, The University of Tokyo

Rheological properties of lower crust are considered to play important roles on the cause of inland earthquakes. Previous studies on creep properties of polycrystalline anorthite indicate that the polycrystalline anorthite will deform under diffusion creep at temperature condition of 400 to 1000C and grain size of <100 um where such conditions are identified in mylonites which are of lower crust origin. Therefore, it is important to know a precise strength of polycrystalline anorthite during diffusion creep.

Previous studies have shown the influence of grain size, temperature, stress, and water content on the strength of polycrystalline anorthite. It is well known that a small amount of impurities segregated at grain boundaries has a significant effect on the strength of polycrystalline oxides. We have shown that our pure anorthite aggregate, which was synthesized using the technique that could minimize the contamination of impurities, had two orders of magnitude larger strength than anorthite aggregates used in previous studies. In this study, we examine the effect of doping a small amount of MgO on high-temperature creep of anorthite aggregates.

MgO-doped anorthite aggregates were fabricated from nano-sized powders of CaCO<sub>3</sub>, Al<sub>2</sub>O<sub>3</sub>, SiO<sub>2</sub>, and Mg(OH)<sub>2</sub>, all of which have <50 nm in diameter, and vacuum sintering of the powders. We controlled the amount of Mg(OH)<sub>2</sub> powders to obtain anorthite doped with 1wt% of MgO. Constant load tests were performed at temperatures ranging from 1150 to 1380C, stresses from 10 to 120 MPa, and confining pressure of 0.1 MPa. We measured Arithmetic mean grain size of specimens by microstructural observations using scanning electron microscopy (SEM) before and after creep tests.

Grain sizes of the specimens were 1~2um before and after the creep test. Log stress versus log strain rate showed a linear relationship where its slope gave a stress exponent, n of 1, indicating that samples were deformed under diffusion creep. MgO-doped anorthite aggregates exhibited more than one order of magnitude weaker than pure anorthite. We obtained activation energy, Q of 702 kJ/mol which was higher than that of our pure anorthite. The difference in strength between pure and MgO-doped anorthite was attributed to the presence of a small amount of MgO which was probably segregated at grain boundaries.

Keywords: polycrystalline anorthite, diffusion creep, effect of doping

## Synthesis of textural polycrystalline forsterite using colloidal processing in a strong magnetic field.

KOIZUMI, Sanae<sup>1\*</sup> ; HIRAGA, Takehiko<sup>1</sup> ; SUZUKI S., Tohru<sup>2</sup> ; SAKKA, Yoshio<sup>2</sup>

<sup>1</sup>Earthquake Research Institute, University of Tokyo, <sup>2</sup>National Institute for Material Science

It is well known that the crystallographic preferred orientation (CPO) of minerals is commonly produced in the Earth's interior. Thus, it is important to understand the physical properties of the mineral aggregates that exhibit CPO. However, silicate minerals are often feeble magnetic and have small anisotropic susceptibilities so that it is difficult to apply a magnetic field effectively to rotate the mineral particles. Tendency of finer particles to spontaneously agglomerate due to strong attractive interactions (van der Waals forces) add further difficulty. We used a technique of slip casting in a high magnetic field (12T) to align certain crystallographic axis of mineral particles. For the particles to rotate easily in the solvent under a strong magnetic field, we improve the method of deflocculating. To control the surface potential of the particles, we applied various types of polymer modification. Vacuum sintering of the powders that were composed of the aligned particles was expected to produce a polycrystalline material aggregate that exhibits CPO. The resultant materials were characterized by X-ray powder diffraction (XRD), secondary electron microscope (SEM) and Electron Backscatter Diffraction (EBSD).

The specimen exposed to a strong magnetic field exhibits preferential A-axis alignment to the magnetic direction. Those synthetic specimens allow us to examine the effect of CPO on the physical properties of the earth's materials in future room experiments.

Keywords: forsterite, polycrystalline, magnetic field, orientation, CPO

## Grain growth experiment on pyrolite material under lower mantle conditions

IMAMURA, Masahiro<sup>1\*</sup> ; KUBO, Tomoaki<sup>1</sup> ; KATO, Takumi<sup>1</sup>

<sup>1</sup>Kyushu Univ.

Grain size is a key parameter for understanding viscosity of Earth's mantle. Grain growth rate is one of important factors controlling the grain size. Especially, it is indispensable to examine grain growth kinetics in multiple phases because the grain growth rate of major phase drastically changes with the proportion of secondary phases (e.g., Hiraga et al., 2010). In the lower mantle, Mg-perovskite is major phase, and ferro-periclase, Ca-perovskite, and majoritic garnet are present as secondary phases (e.g., Irifune, 1994; Nishiyama and Yagi, 2003). The previous grain growth experiment (Yamazaki et al., 1996) in the two-phase system of MgSiO<sub>3</sub> perovskite and MgO periclase using Mg<sub>2</sub>SiO<sub>4</sub> forsterite as a starting material suggests that the grain growth rate is too slow to explain the lower mantle viscosity constrained by geophysical observations. This inconsistency may arise from effects of the eutectoid transformation prior to the grain growth process (e.g., Solomatov et al., 2002). It is also necessary to examine effects of the chemical composition that affects the proportion of secondary phases and diffusivity. Here, we report preliminary results of the grain growth experiment on pyrolite material under lower mantle conditions.

High-pressure and temperature experiments were conducted using a Kawai-type multi-anvil apparatus (QDES) installed at Kyushu University. Starting material is a powder with pyrolite composition that was used in the previous phase equilibrium study (e.g., Irifune, 1994). We conducted annealing experiments at 25-28 GPa and 1600-1800 °C for 6-600 min. Chemical compositions, microstructures and grain sizes of recovered samples were examined using a FE-SEM with an energy-dispersive analytical system.

Four phases of Mg-perovskite, Ca-perovskite, ferro-periclase and majoritic garnet were present in recovered samples annealed at 25 GPa and 1600-1800 °C. The normalized grain size distribution in the recovered samples showed Gaussian-like shape and the largest grain size is smaller than three times of the mean grain size, suggesting that normal grain growth occurred. The grain growth rate is faster than that of the previous study (Yamazaki et al., 1996). Preliminary analysis of the kinetic data of Mg-perovskite obtained showed the smaller grain growth exponent of 4.3 than that reported in the previous study. On the other hand, three phases of Mg-perovskite, Ca-perovskite and ferro-periclase were present at higher pressure of 28 GPa and 1800 °C, in which the volume fraction of Mg-perovskite increased compared to the four-phases experiment. While the microstructure and the grain size distribution in the three-phase assemblage was similar to those of the four-phase assemblage, the grain size was larger probably due to the smaller proportion of the secondary phases. Our preliminary results provide some insights into the grain-size evolution in the lower mantle and suggest that further quantitative grain growth data with possible lower mantle conditions are needed.

Keywords: lower mantle, multi-anvil, pyrolite, grain growth

## Grain boundary diffusion of noble metal elements in mantle composites

MATSUO, Naoya<sup>1\*</sup> ; HIRAGA, Takehiko<sup>1</sup>

<sup>1</sup>Eartuquake Research Institute, The University of Tokyo

So far, it is not clear whether Earth's core and mantle have been chemically isolated through geological time. It has been believed that highly incompatible elements such as siderophile elements in the mantle minerals have not been moved from the core to the mantles so that the elemental abundance of highly siderophile elements (HSEs) in the core and mantle were determined when both were separated. Although HSEs are refractory, amounts of HSEs are very little in the mantle (Wood, 2006) so that these elements are expected to be highly concentrated in the core relative to the silicate mantle. However, a recent study has shown that incompatible elements can be concentrated and quickly diffuse at grain boundaries (Hiraga et al., 2004). If HSEs can diffuse from the core to the mantle, the concentration of HSEs in the mantle can change through Earth's history. Therefore, HSEs can be a good tracer to detect the chemical interaction of the core and the mantle.

We conducted grain growth experiments on Au particles in forsterite (Fo) aggregates at 1 atmosphere pressure and temperature of 1360 °C. We prepared several sintered bodies which were made by dispersing 10vol% Au particles in Fo aggregates and then annealed for several hours. We observed these bodies using a scanning electronic microscope. In the result, Au particles changed their shape from spherical to polygonal. This is due to a balance of interfacial tensions between Au and Fo phases. Further, average grain size of Au particles was found to increase with time. Based on these observations, we conclude that Ostwald ripening of grains, by which Au atoms move from small particles to larger ones to minimize entire interfacial energies of the system, occurred in our experiment. Grain boundaries as diffusion paths should be responsible for Au diffusion. In this case, grain growth of Au particles will follow the relationship of  $d^4 - d_0^4 = kt$ , where  $d$  is the average grain size of Au particles after annealing,  $d_0$  is the initial average grain size,  $k$  is the grain growth coefficient, and  $t$  is annealing time. Using the average grain size of each body, we calculated  $k$ . In addition, we estimated the interfacial energy of the system from the shape of Au particles and calculated the product of concentration of Au particles at grain boundaries,  $c$ , and diffusivity of Au atoms at grain boundaries,  $D$ .

Keywords: grain boundary diffusion, grain growth, core-mantle interaction

## The effect of partial melting on the mantle viscosity and electrical

SUEYOSHI, Kenta<sup>1\*</sup>; HIRAGA, Takehiko<sup>1</sup>

<sup>1</sup>Earthquake Research Institute, University of Tokyo

In this study, in order to know the change in mantle viscosity and electrical conductivity during partial melting, which corresponds to decompression melting of ascending mantle beneath mid-ocean ridge, mantle analogue sample was synthesized and used to measure its viscosity and electrical conductivity under atmospheric pressure and high temperature conditions. The sample has lherzolite composition of olivine (50%), orthopyroxene(40%) and clinopyroxene(10%) with addition of 0.5 vol% spinel. Constant force was applied to the sample under increasing the temperature where its range includes sample solidus. Sample viscosity and the electrical conductivity by the impedance measurement were calculated for every temperature. We particularly examined how viscosity and conductivity change when the sample transforms from melt-free to melt-bearing system. Temperature ranged from 1100 to 1390 °C, which resulted in the change of melt fraction ( $\phi$ ) from 0 to 0.09, where the melt composition becomes enriched in clinopyroxene component as the temperature increases.

We observed a continuous and gradual reduction of sample viscosity with increasing temperature. The effect of the increasing melt fraction on the sample viscosity should have been added to the viscosity change simply due to thermally activation process. There is a linear relationship between measured  $1/T$  and  $\log(1/\eta)$ , which goes well with the previous proposed empirical expression of flow law that, which is an function of melt fraction.

Analyzing the observed viscosity change with temperature with this law, the apparent activation energy of 970 kJ/mol is obtained at a temperature range of 1220 °C to 1340 °C and the effect of increasing melt fraction on sample viscosity roughly corresponds to the activation energy of  $\sim$ +35 kJ/mol. The activation energy on the melt free system is estimated to be 935 kJ/mol. This value is close to the activation energy of the dislocation creep of orthopyroxene and clinopyroxene indicating that the sample viscosity was essentially controlled by deformation of pyroxenes.

Electrical conductivity did not change dramatically when the experimental temperature reached and exceeded the sample solidus. Grain size dependency on the conductivity was observed at all temperature conditions indicating that the conductivity is simply determined by grain boundary conductivity even at higher melt fraction condition, probably due to fine grain size of the samples. Compared with previously reported grain boundary conductivity in the melt-free forsterite system, grain boundaries in our sample have 3 to 4 times higher conductivity indicating that the pyroxene grain boundaries have a large effect on the bulk sample conductivity in our experiment.

In this study, it was demonstrated that previously proposed empirical flow law as a function of melt fraction can approximate the viscosity change of the mantle during its transition from melt-free to melt-bearing. Taking into account of the incremental rate of melt fraction with temperature and the connectivity of intergranular melt in the mantle highly depend on the volume fraction of the pyroxenes and spinel phases, mineral mode in the mantle should have substantial effects on the mantle rheology and electrical conductivity during mantle melting.

Keywords: rheology, lherzolite, melt, viscosity, electrical conductivity

## Stress calibration of Griggs-type deformation apparatus with solid salt assemblies

KIDO, Masanori<sup>1\*</sup> ; MUTO, Jun<sup>1</sup> ; NAGAHAMA, Hiroyuki<sup>1</sup>

<sup>1</sup>Department of Earth Sciences, Tohoku University

Mechanical properties of rocks and minerals can be quantitatively studied by deformation experiments under high-temperature and high-pressure conditions relevant to the Earth's interior. There are several types of deformation apparatus using different confining media such as gases, liquids or weak solids (e.g., Tullis and Tullis, 1986). Liquid medium apparatus have the disadvantage that they cannot be used for temperatures above 500 °C because of prevention from alteration of oil at high temperature. Solid medium apparatus can provide us high pressure safely and stably for a long time. However, stress accuracy is not high due to frictional forces between pressure medium and load piston or samples (e.g., Tullis and Tullis, 1986). Gas apparatus has most accurate stress measurement because of the usage of internal load cell; thus measured stresses do not include frictional forces. However, experiments are restricted to confining pressures less than 200 MPa in Japan due to safety issues on the usage of high-pressure gas. Therefore, solid medium apparatus is necessary for generating high temperature and high pressure required to investigate rheological behaviors of rocks and minerals in lower crust or uppermost mantle.

Recently, comparisons of mechanical results obtained for metals at the same confining pressure, temperatures and strain rates deformed in a Griggs apparatus with solid salt assemblies (SSA) and a gas apparatus provide calibration for Griggs apparatus with SSA (Holyoke and Kronenberg, 2010). This calibration law allowed differential stresses to be measured accurately to within  $\pm 30$  MPa. However, we have not been able to reproduce elastic, yielding and post-yield behaviors because the calibration law was obtained by the comparison of strengths at 5% strain of mechanical results. Calibration law for measured stresses using Griggs apparatus in all deformation behaviors are required for revealing detailed rheological behavior of rocks and minerals.

In this study, we performed axial compression experiments on high-purity nickels to measure differential stresses using a Griggs apparatus with SSA at Tohoku University. Samples were given by Drs. Holyoke and Kronenberg. Experimental conditions were confining pressures of 300 and 1200 MPa, temperatures of 600, 700, and 800 °C and strain rates of  $2 \times 10^{-4}$ ,  $2 \times 10^{-5}$  and  $2 \times 10^{-6}$  /s. Measured differential stresses agreed with results of the former study within  $\pm 30$  MPa under the identical confining pressure of 300 MPa. However, differential stresses were larger with confining pressure. We analyzed obtained mechanical data of nickels based on the high temperature viscoelastic constitutive law developed by Shimamoto (1987). We made the master curve which normalized temperature and strain conditions. In the same way, we also made the master curve from mechanical data of nickels using a gas apparatus (mechanical data are from Holyoke and Kronenberg, 2010). Master curves were made of mechanical data of the identical material between Griggs apparatus and gas apparatus under normalized temperature and strain conditions. Therefore, difference in master curves is thought to be derived from apparatus and assembly. We derived calibration law for Griggs apparatus from difference in master curves. Applying this calibration law to differential stresses of nickels obtained using Griggs apparatus with SSA, it became possible to reproduce gas apparatus's differential stresses not only steady state but also elastic, yield and post-yield behaviors within the systematic error of  $\pm 30$  MPa. However, the error was  $\pm 70$  MPa when the calibration law was applied to the mechanical data of carbonate rock. Moreover, unlike gas apparatus, measured differential stresses using Griggs apparatus tend to become larger with confining pressures. Therefore, it is necessary to investigate the effect of confining pressures on measured stresses in the calibration law.

Keywords: rheology, deformation experiment, calibration of Griggs-type apparatus

## Preliminary experiments on in-situ stress-strain measurements of Ca-Pv and Mg-Pv up to 23 GPa

TSUJINO, Noriyoshi<sup>1\*</sup> ; YAMAZAKI, Daisuke<sup>1</sup> ; YOSHINO, Takashi<sup>1</sup> ; SAKURAI, Moe<sup>2</sup> ; NISHIHARA, Yu<sup>3</sup> ; HIGO, Yuji<sup>4</sup>

<sup>1</sup>ISEL, Okayama Univ., <sup>2</sup>Tokyo tech., <sup>3</sup>GRC, Ehime Univ., <sup>4</sup>JASRI

In order to discuss mantle dynamics in the Earth's interior, knowledge of viscosity of the Earth's lower mantle, which is the highest of the whole mantle, is important. Viscosity models of the Earth's lower mantle were reported by geophysical observations. However, observation values of viscosity have large variety (2~3 order magnitude). Although determination of viscosity of lower mantle minerals by high pressure experiments is needed to understand mantle dynamics, stress-strain relationship for MgSiO<sub>3</sub>-perovskite (Mg-Pv) and CaSiO<sub>3</sub>-perovskite (Ca-Pv), which are principal minerals of the Earth's lower mantle, are not reported due to difficulty of high pressure deformation experiments. In this study, we tried in-situ stress-strain measurements of Ca-Pv and Mg-Pv up to 23.0 GPa.

In-situ uniaxial deformation experiments were conducted using a deformation DIA apparatus (SPEED-Mk.II) as Kawai-type apparatus at SPring-8 BL04B1. Experimental conditions of Ca-Pv and Mg-Pv are 13.8 GPa, 1473 K and 23.0 GPa, 1273 K, respectively. cBN anvils, which was transparent material against X-ray, was used along X-ray path. Two-dimensional X-ray diffraction patterns were taken for 120-180 s using CCD detector. To calculate the stress magnitude from the X-ray diffraction data, we used a model of stress-lattice strain relationship (Singh et al. 1998),

$$d_{hkl}(\psi) = d_{0hkl} [1 + (1 - 3\cos^2\psi) \sigma / 6 G_{hkl}] \quad (1)$$

where  $d_{hkl}$  is the d-spacing measured as a function of azimuth angle  $\psi$ ,  $d_{0hkl}$  is the d-spacing under the hydrostatic pressure,  $G_{hkl}$  is the appropriate shear modulus for a given hkl, and  $\sigma$  is the uniaxial stress. Pressure and stress were estimated using Ca-Pv (110) (200) and Au (111) diffraction in Pressure marker (Au : Fo = 1 : 2 volume ratio) at deformation experiments of Ca-Pv and Mg-Pv, respectively. An X-ray radiograph of the strain markers was taken using an imaging system composed of a YAG crystal and a CCD camera with an exposure time of 60 s.

Uniaxial stress of Ca-Pv at 13.8 GPa, 1473 K and  $\sim 1.2 \times 10^{-5}$  /s and Mg-Pv at 23.0 GPa, 1273 K and  $\sim 1.5 \times 10^{-5}$  /s were estimated as  $\sim 2$  GPa and  $\sim 0.25$  GPa, respectively. Stress of Mg-Pv was significantly smaller than that of Ca-Pv though temperature condition of Mg-Pv was lower than that of Ca-Pv. This fact is doubtful. This reason is thought that stress estimated by Au was much smaller than that of Mg-Pv because of framework made by Ringeoodite, which was polymorphic phase of Fo in pressure marker.

Keywords: In-situ measurements, deformation experiments, Stress, Strain, Perovskite, The Earth's lower mantle